

# Cone-setting in spruce is regulated by conserved elements of the age-dependent flowering pathway

Shirin Akhter<sup>1\*</sup> , Karl Johan Westrin<sup>2\*</sup> , Nathan Zivi<sup>1,3\*</sup>, Veronika Nordal<sup>1</sup>, Warren W. Kretschmar<sup>2</sup> , Nicolas Delhomme<sup>4</sup> , Nathaniel R. Street<sup>5</sup> , Ove Nilsson<sup>4</sup> , Olof Emanuelsson<sup>2</sup>  and Jens F. Sundström<sup>1</sup> 

<sup>1</sup>Department of Plant Biology, Linnean Center for Plant Biology, Uppsala BioCentre, Swedish University of Agricultural Sciences (SLU), SE-750 07 Uppsala, Sweden; <sup>2</sup>Science for Life Laboratory, Department of Gene Technology, KTH Royal Institute of Technology, SE-171 65 Solna, Sweden; <sup>3</sup>Skogforsk, Uppsala Science Park, Uppsala SE-751 83, Sweden; <sup>4</sup>Department of Forest Genetics and Plant Physiology, Umeå Plant Science Centre, Swedish University of Agricultural Sciences (SLU), SE-901 83 Umeå, Sweden; <sup>5</sup>Department of Plant Physiology, Umeå Plant Science Centre, Umeå University, SE-901 87 Umeå, Sweden

## Summary

Authors for correspondence:  
Olof Emanuelsson  
Email: olofem@kth.se

Jens F. Sundström  
Email: jens.sundstrom@slu.se

Received: 28 May 2022  
Accepted: 23 August 2022

New Phytologist (2022) 236: 1951–1963  
doi: 10.1111/nph.18449

**Key words:** cone-setting, flowering, gymnosperm, *Picea abies*, reproductive development, SPL-gene family, transcriptome.

- Reproductive phase change is well characterized in angiosperm model species, but less studied in gymnosperms. We utilize the early cone-setting *acrocona* mutant to study reproductive phase change in the conifer *Picea abies* (Norway spruce), a gymnosperm. The *acrocona* mutant frequently initiates cone-like structures, called transition shoots, in positions where wild-type *P. abies* always produces vegetative shoots.
- We collect *acrocona* and wild-type samples, and RNA-sequence their messenger RNA (mRNA) and microRNA (miRNA) fractions. We establish gene expression patterns and then use allele-specific transcript assembly to identify mutations in *acrocona*. We genotype a segregating population of inbred *acrocona* trees.
- A member of the *SQUAMOSA BINDING PROTEIN-LIKE (SPL)* gene family, *PaSPL1*, is active in reproductive meristems, whereas two putative negative regulators of *PaSPL1*, *miRNA156* and the conifer specific *miRNA529*, are upregulated in vegetative and transition shoot meristems. We identify a mutation in a putative *miRNA156/529* binding site of the *acrocona PaSPL1* allele and show that the mutation renders the *acrocona* allele tolerant to these miRNAs. We show co-segregation between the early cone-setting phenotype and trees homozygous for the *acrocona* mutation.
- In conclusion, we demonstrate evolutionary conservation of the age-dependent flowering pathway and involvement of this pathway in regulating reproductive phase change in the conifer *P. abies*.

## Introduction

Molecular clock-based studies, calibrated using fossil data, suggest that the gymnosperm and angiosperm lineages of extant seed plants separated *c.* 300 million years ago (Smith *et al.*, 2010). Although the lineages share a common feature in the seed, their seed-bearing structures differ. Gymnosperms form seed- and pollen-bearing structures from separate shoot meristems, commonly referred to as cones (Florin, 1951) whereas angiosperm flowers, in their ancestral state, are bisexual (Sauquet *et al.*, 2017). Cones and flowers also differ in their branching order (Florin, 1951), where at least seed cones can be viewed as reproductive shoots analogous to angiosperm inflorescences, rather than flowers.

Comparative studies indicate that the genetic mechanisms that determine male or female organ identity are conserved between the two lineages (Rutledge *et al.*, 1998; Tandre *et al.*, 1998;

Mouradov *et al.*, 1999; Sundstrom *et al.*, 1999; Winter *et al.*, 1999). However, it is currently disputed if the mechanisms that regulate the on-set of cone-setting in gymnosperms and flowering in angiosperms are homologous (Karlgrén *et al.*, 2011; Klintenas *et al.*, 2012; Liu *et al.*, 2016).

Angiosperm flowering is regulated by several independent pathways that act in parallel, and converge on common floral integrators (O'Maoileidigh *et al.*, 2014). The pathways are often referred to as the Age-dependent pathway, the Day-Length pathway, the Hormonal pathway, and the Vernalization pathway (Blazquez & Weigel, 2000). The transition from vegetative growth to flowering occurs once in annual plants but can occur repeatedly in perennials (Albani & Coupland, 2010). The repeated flowering of the perennial herb *Arabidopsis thaliana* can be explained by the regulation of transcription factor proteins belonging to the SQUAMOSA BINDING PROTEIN-LIKE (SPL) family (Hyun *et al.*, 2019). SQUAMOSA BINDING PROTEIN-LIKE proteins act as activators of flowering through the regulation of flower meristem identity genes (Wang

\*These authors contributed equally to this work.

*et al.*, 2009). *Arabidopsis thaliana* *SPL15* transcript levels are negatively regulated in vegetative meristems through the joint activity of factors involved in the Vernalization pathway and the age-dependent pathway. In response to winter temperatures and vernalization, the repression of *SPL15* is temporarily lifted. Flowering is allowed to occur, but only in meristems that have reached a certain age, since *SPL15* is also negatively regulated by the Age-dependent pathway through the activity of *micro-RNA156* (*miR156*; Hyun *et al.*, 2019).

Like many conifers, wild-type *Picea abies* trees go through a long juvenile period of 20–25 yr before initiating cones. Thereafter, cone-setting occurs every third to fifth year (Lindgren *et al.*, 1977). To study cone-setting, we use a naturally occurring *P. abies* mutant called *acrocona*. Homozygous *acrocona* plants display a recessive early cone-setting phenotype and initiate cones already in their second growth period (Uddenberg *et al.*, 2013). After the first cone-setting, *acrocona* trees also initiate cones frequently, almost every year. This frequent cone-setting phenotype is semi-dominant and can to a degree also be observed in adult heterozygous *acrocona* mutants. In addition, heterozygous *acrocona* mutants commonly form cone-like structures, called transition shoots, on leading vegetative branches (Carlsbecker *et al.*, 2013; Uddenberg *et al.*, 2013).

Massively parallel DNA sequencing has been employed to study different aspects of reproductive development in conifers by us (Uddenberg *et al.*, 2013; Giacomello *et al.*, 2017) and others (Niu *et al.*, 2014, 2016; Futamura *et al.*, 2019). Previously, we have studied inbred siblings of young *acrocona* trees (Uddenberg *et al.*, 2013) and identified the MADS-box gene *DEFICIENS AGAMOUS LIKE 19* (*DAL19*) as being upregulated in needle samples of early cone-setting shoots. Later we have shown that distinct *DAL19* isoforms are expressed in male and female cones, and in vegetative shoots (Akhter *et al.*, 2018).

In the present study, we take advantage of the transition shoots and the numerous female cones that regularly form on adult heterozygous *acrocona* trees, and during cone-years also in the upper one-third of adult wild-type *P. abies* trees. We use massively parallel DNA sequencing to analyse both the messenger RNA (mRNA) and microRNA (miRNA) fractions of early meristems and transition shoot primordia from *acrocona* and compare those to corresponding samples from wild-type vegetative shoots and female cones. We hypothesize that candidate genes active in these early meristems are important not only for the *acrocona* phenotype but also for the regulation of cone-setting in wild-type *P. abies*. In line with this hypothesis, we identify candidates for a cone-setting regulatory circuit consisting of a conifer SPL-gene family member and two miRNAs. Furthermore, by genotyping a segregating sibling population of inbred *acrocona* trees, we provide evidence for a functional link between a mutation in a candidate gene, *PaSPL1*, and the early cone-setting *acrocona* phenotype.

## Materials and Methods

### Plant materials and morphological conditions

Plant material was collected from an *acrocona* tree located in Uppsala, Sweden and from a wild-type Norway spruce (*P. abies*

(L.) H. Karst.) at the Rörby seed orchard (latitude 59°54'290''N) near Uppsala, Sweden. Both trees were estimated to be at least 50 yr. Samples representing two developmental stages were collected from both genotypes. In the first developmental stage, the samples consisted of meristematic tissue. Samples in the second developmental stage harboured bud primordia with differentiating lateral organs. The *acrocona* samples consisted of transition shoots collected from apical positions on leading branches and female cones collected from apical positions on lateral branches. The *acrocona* samples used in RNA-sequencing (RNA-Seq) experiments were collected at two dates in 2016, 1 August and 18 October. Whereas the corresponding wild-type samples consisted of vegetative shoots collected from apical positions on leading branches and female cones collected from apical positions on lateral branches. Wild-type samples were collected in 2016, on 1 August, 16 September, and 25 October. Independent control samples of female cones and vegetative shoots were also collected from four additional wild-type genotypes on 8 October 2013. All plant materials used for RNA preparations were snap-frozen in liquid nitrogen and stored at  $-70^{\circ}\text{C}$ . For a summary of the sample information and a detailed description of the sampling procedure, see Table S1.

### RNA preparation

Tissue homogenization, extraction, CHISAM (chloroform/isoamylalcohol, 24 : 1) purification and isopropanol precipitation were performed as described by Azevedo *et al.* (2003). Harvested RNA pellets were dissolved in 350  $\mu\text{l}$  RLT buffer (Qiagen RNeasy Kit; Qiagen, Carlsbad, CA, USA). Separate miRNA-enriched fractions (<200 nt) and total RNA fractions were purified from each RNA sample using the RNeasy MinElute Cleanup Kit (74204; Qiagen) following manufacturer's instructions. RNA integrity was assessed via Bioanalyzer (Agilent Technologies, Santa Clara, CA, USA) and NanoDrop ND-1000 Spectrophotometer (ThermoFisher Scientific, Waltham, MA, USA). All RNA samples used for sequencing and subsequent molecular analyses had an RNA Integrity Number (RIN) between seven and nine.

### Library preparation and RNA-sequencing (mRNA)

Sequencing libraries were prepared from 500 ng total RNA using the TruSeq stranded mRNA library preparation kit (RS-122-2101/2102; Illumina Inc., San Diego, CA, USA) including polyA selection. The library preparation was performed according to the manufacturer's protocol (#5031047). A  $2 \times 125$  bp short-read paired-end RNA-Seq of all bud samples was performed using a HiSeq2500 with v4-sequencing chemistry by The SNP & SEQ Technology Platform in Uppsala, Sweden.

### Pre-processing of RNA-sequencing data: quality control, gene quantification (mRNA)

The data pre-processing was performed following the guidelines described in <http://www.epigenesys.eu/en/protocols/bio-informatics/1283-guidelines-for-rna-seq-data-analysis>. Briefly, the quality of

the raw sequence data was assessed using FASTQC (<http://www.bioinformatics.babraham.ac.uk/projects/fastqc/>), v.0.11.4. Residual ribosomal RNA (rRNA) contamination was assessed and filtered using SORTME RNA (v.2.1; Kopylova & No, 2012). Data were then filtered to remove adapters and trimmed for quality using TRIMMOMATIC (v.0.36; Bolger *et al.*, 2014). After both filtering steps, FASTQC was run again to ensure that no technical artefacts were introduced. Read counts were obtained using KALLISTO (v.0.43.0; Bray *et al.*, 2016) using the *P. abies* v.1.0 complementary DNA (cDNA) sequences as a reference (retrieved from the PlantGenIE resource (Sundell *et al.*, 2015)). The KALLISTO abundance values were imported into R (v.3.4.0; R\_Core\_Team, 2013) using the BIOCONDUCTOR (v.3.4; Gentleman *et al.*, 2004) TXIMPORT package (v.1.4.0; Soneson *et al.*, 2015). For the data quality assessment (QA) and visualization, the read counts were normalized using a variance stabilizing transformation as implemented in the BIOCONDUCTOR DESEQ2 package (v.1.16.1; Love *et al.*, 2014).

### Principal component analysis and differential gene expression analysis

Principal component analysis (PCA) was conducted in R 3.5.0 using the built-in R function `prcomp` on normalized read count data. The PCA was performed on the complete set of expressed genes in the sequenced materials to check biological relevance of the data. We plotted the first three PCA three dimensions using CRAN package `SCATTERPLOT3D` v.0.3-41. We performed differential expression analysis on the normalized read counts using a negative binomial distribution as implemented in DESEQ2 v.1.16.1. (Love *et al.*, 2014). The threshold to judge the significance of gene expression differences was false discovery rate (FDR)  $\leq 0.01$  and the absolute value of  $\log_2$ FoldChange ( $\log_2$ FC)  $\geq 0.5$  as per the recommendation from Schurch *et al.* (2016). The package `VENNDIAGRAM` was used to create a venn-diagram of differentially expressed genes (DEGs).

### Cloning of full-length complementary DNA clones

To verify the presence of full-length transcripts we synthesized cDNA libraries using M-MLV Reverse Transcriptase (28025013; Invitrogen) and 500 ng of total RNA derived from female cones as template. The cDNA was used in a PCR-reaction (1  $\times$  98°C for 3 min, 35  $\times$  (98°C for 10 s, 61°C for 30 s, 72°C for 2 min), 72°C for 12 min) to amplify the sequence corresponding to the open reading frame of PaSPL1 using primers listed in Table S2a and Phusion High-Fidelity DNA Polymerase (F530L; ThermoFisher Scientific). The amplified PCR-product was subsequently cloned into a Zero Blunt TOPO (K2800J10; Invitrogen) cloning vector and sent to Eurofins Genomics (Ebersberg, Germany) for Sanger *et al.* (1977) sequencing.

### Reverse transcription quantitative polymerase chain reaction

Reverse transcription quantitative polymerase chain reaction (RT-qPCR) amplifications were performed as described in

Akhter *et al.* (2018). Gene specific primers were designed using the Primer3 algorithm implemented in GENEIOUS PRO v.10.2.3 created by Biomatters Ltd, Auckland, New Zealand; <http://www.geneious.com>. All primers used in this study amplified with an efficiency between 85 and 110% (Table S2b). Gene expression was measured in three biological samples of each tissue type. All biological samples were analysed in duplicate. The expression data of each gene were normalized against the expression of three reference genes, *ACTIN*, *POLYUBIQUITIN*, and *HISTONE2A*. Calculations and normalizations were done using the CFX software based on the  $\Delta C_t$  or  $\Delta\Delta C_t$  methods (Bio-Rad, Hercules, CA, USA). Statistical analyses were performed using R v.3.4.2.

### Phylogenetic analysis

Annotated *SPL* genes from *P. abies*, *Arabidopsis thaliana* and *Populus trichocarpa* were included in the analysis. For each gene, the coding sequences were translationally aligned using the MAFFT module in GENEIOUS (GENEIOUS v.10.2.3; Biomatters Ltd, Auckland, New Zealand) and the resulting alignments were curated using the BMGE software with default settings (Criscuolo & Gribaldo, 2010). Phylogenetic analysis was carried out using MRBAYES v.3.2.6 (Huelsenbeck & Ronquist, 2001).

### Library preparation and RNA-sequencing (miRNA)

Sequencing libraries were prepared from the fraction of small (< 200 nt) RNAs resulting from the RNA preparation using the TruSeq small RNA library preparation kit (RS-200-0012; Illumina Inc.) according to the manufacturer's protocol. A 2  $\times$  50 bp short-read paired-end RNA-Seq of all bud samples were performed using a NovaSeq SP-100 by the SNP & SEQ Technology Platform in Uppsala, Sweden.

### Pre-processing of RNA-sequencing data: quality control, gene quantification (miRNA)

Small RNA fraction RNA-Seq reads were pre-processed by means of quality pruning and adapter trimming using FASTP (Chen *et al.*, 2018) with the default settings, resulting in a set of high-quality reads.

We used the miRNA database miRBase release 22.1 to match high-quality reads with known miRNAs (Kozomara *et al.*, 2019) originating from *P. abies*, *A. thaliana* and *Populus trichocarpa*. We used KALLISTO to estimate miRNA abundance levels (both estimated counts and transcript per million (TPM)) by creating an index of 19-mers and 100 bootstrap samples during the actual quantification (Bray *et al.*, 2016). We used sleuth to perform differential expression analysis of miRNAs (Pimentel *et al.*, 2017). In sleuth, we used the likelihood ratio test (LRT) to detect differential expression and excluded miRNAs with a *q*-value larger than 0.05 from further analyses.

### Transcriptome reconstruction

We used CLUSTRACT (Westrin *et al.*, 2022) with default settings (and using the built-in approach to generate the so-called guiding

contigs it requires) to generate a *de novo* assembly of the entire transcriptome. We included all the samples from 1 August in the assembly and aligned the *de novo* assembled transcripts to the *P. abies* reference genome (*P. abies* v.1.0) using MINIMAP2 (Li, 2018), with the preset option 'splice:hq'.

Since several of the *de novo* assembled transcripts mapped sequentially to several ConGenIE scaffolds (MAs) we used this information to connect the exon sequences of genes that mapped to multiple scaffolds in the current genome assembly. Each reference sequence was counted for only once.

### Allele specific assembly

To identify single nucleotide polymorphisms (SNPs) in candidate genes, we performed separate *de novo* assemblies using linked De Bruijn graphs (Turner *et al.*, 2018) combined with KALLISTO (Bray *et al.*, 2016), as outlined in Akhter *et al.* (2018). The method has since been named Abeona and is available at: <https://github.com/winni2k/abeona>.

### Genotyping

Genomic DNA was extracted from tissue samples using a CTAB protocol (Kim *et al.*, 1997). PCR-fragments covering *acrocona* specific SNPs were PCR-amplified using 100 ng of genomic DNA as template, Phusion DNA Polymerase (F-530; ThermoFisher Scientific) and primers listed in Table S2a. The resulting PCR-products were purified using the QIAquick PCR Purification Kit according to manufacturer's instructions (28104; Qiagen) and sent to Eurofins Genomics for Sanger *et al.* (1977) sequencing. The presence of a polymorphism was detected as double peaks in the resulting ab1-files (Fig. S1).

### Allele specific expression analysis

The *PaSPL1* alleles were used to generate an index for KALLISTO, which we used to run each mRNA sample on. In the output, we could detect the allele frequencies from the TPM values, presented as average allele frequency across three biological samples.

### *PaSPL1* transcript degradation estimated by 5' RLM RACE

RNA Ligase-Mediated 5' Rapid Amplification of cDNA Ends (RLM RACE) was performed essentially as described by Llave *et al.* (2011). Samples used in the RLM RACE experiments are listed in Table S3. Briefly, RNA oligonucleotide adaptors were ligated to the 5' terminus of cleaved transcripts using T4 RNA ligase (EL0021; ThermoFisher Scientific). The ligated RNA samples were subsequently reverse transcribed into first-strand cDNA using Superscript IV Reverse Transcriptase (18090010; Invitrogen). To amplify *PaSPL1* degradation products, we performed a primary touch-down PCR, followed by a nested secondary PCR using Phusion DNA Polymerase (F-530, ThermoFisher Scientific) and primers listed in Table S2c. The resulting PCR products were size separated on an agarose gel, cloned into Zero Blunt TOPO cloning vector (K22800J10; Invitrogen) and transformed

into chemically competent OneShot TOP10 *Escherichia coli* cells (C404010; Invitrogen). Transformed cells were pre-screened for the presence of the *PaSPL1* sequence using colony PCR, and selected clones were sent to Eurofins Genomics for Sanger sequencing (Sanger *et al.*, 1977).

To quantify the *PaSPL1* degradation products, we performed qPCR experiments using Maxima SYBR Green qPCR Master Mix (KO221; ThermoFisher Scientific) and *PaSPL1* specific primer pairs (Table S2c). PCR fragments were quantified on a CFX Connect Real-Time PCR Detection System (Bio-Rad). The relative abundance of *PaSPL1* degradation products was normalized against the  $C_t$  value of the 5'-fragment in each sample, as outlined by Muller *et al.* (2002).

## Results

### Apical buds on leading branches formed *acrocona* transition shoots

In order to identify genes important to the *acrocona* transition shoot phenotype we sequenced the mRNA fraction of samples collected from leading shoots and lateral shoots (Fig. 1a) on branches situated in the cone-setting region of two *P. abies* genotypes: an *acrocona* mutant and a wild-type comparator. Lateral shoot meristems produced female cones in both wild-type *P. abies* and in the *acrocona* mutant (Fig. 1b,d) whereas leading shoot meristems produced vegetative shoots in the wild-type and transition shoots in the *acrocona* mutant (Fig. 1c,d).

We collected samples at the initiation of bud development and when the buds had started to differentiate. The buds harboured enlarged shoot apical meristems with only a few or no lateral organs at the early time-point. The later samples bore bud primordia with differentiating lateral organs while only a small meristem remained. Wild-type vegetative shoots initiated needles, whereas female shoots from both genotypes produced bracts and ovuliferous scales. In the *acrocona* transition shoots, needles had been formed in the basal part of the shoot, and bracts and ovuliferous scale-like structures had been formed in the apical part of the shoot (Fig. 1d).

### Fourteen genes were commonly upregulated in *acrocona* transition shoots and female shoots

A PCA was carried out to analyse the relationships between samples and mRNA transcription profiles (Fig. 2a). The first principal component (PC1) explained 48% of the total variation, and samples grouped according to collection dates along this axis (Fig. 2a). The second principal component (PC2) explained 15% of the variation in the samples. Notably, all *acrocona* samples grouped close to each other along this axis and were distinct from wild-type bud samples (Fig. 2a). Thus, the samples formed distinct groups and the grouping could be attributed to collection date (i.e. growth phase) and genotype.

We identified mRNA transcripts with a significant difference in expression levels in at least one of three sample types (*acrocona* transition shoots, *acrocona* and wild-type female shoots) as

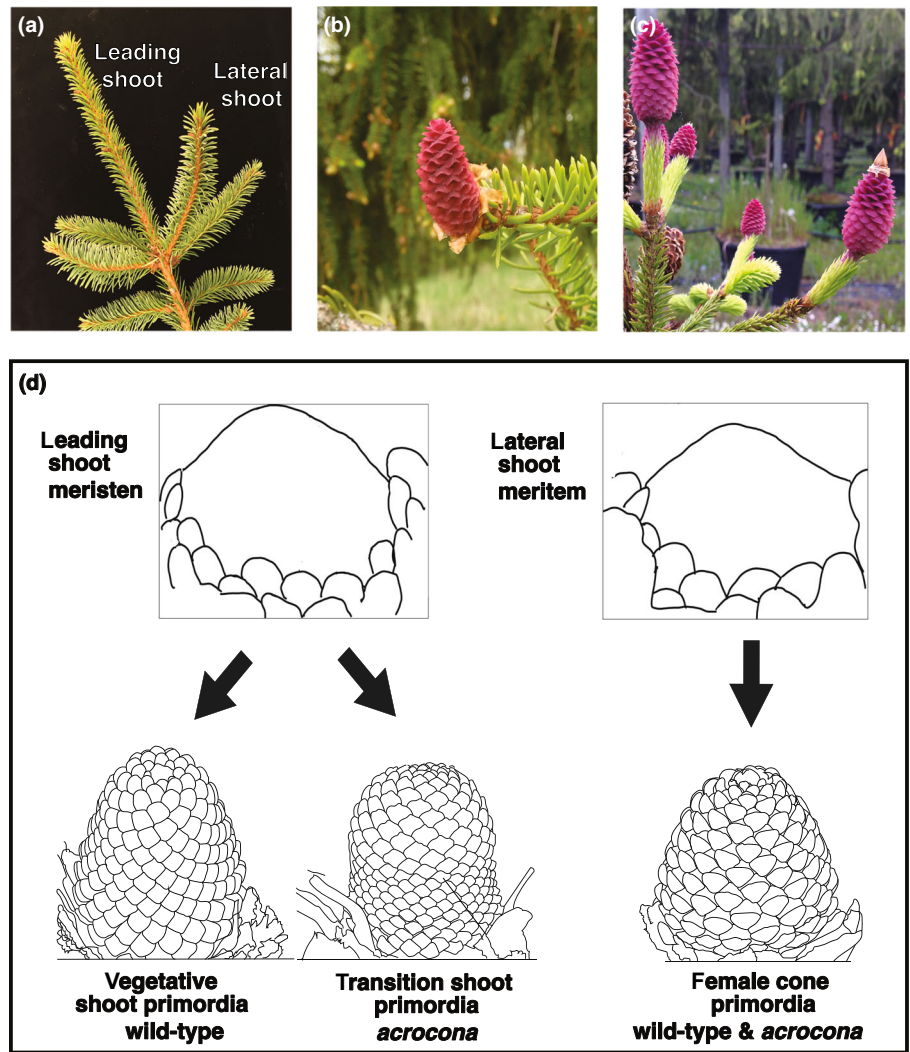


**Fig. 1** Illustration of female cones, vegetative shoots and *acrocona* transition shoots. Shown in (a) is a branch of *Picea abies*, with the leading shoot and lateral shoots indicated. The pictures show a mature female cone in (b) and mature *acrocona* transition shoots in (c). The drawings in (d) illustrate the tissue types sampled in this study. Leading shoot meristems develop into vegetative (Veg) shoot primordia in wild-type, and into transition shoot (TS) primordia in the *acrocona* mutant. Lateral shoot meristems develop into female (F) cones primordia in both wild-type *Picea abies* and the *acrocona* mutant.

compared to the base-line sample (wild-type vegetative leading shoots). We did this separately for both meristem (early) and primordia (late) samples. In total 8407 genes were significantly differentially expressed between buds collected in the early developmental stages (Fig. 2b). Among those, 515 genes were either upregulated or downregulated in all three comparisons (Figs 2b, S2; Dataset S1). Similarly, a total of 10 542 genes were significantly differentially expressed between bud samples collected in the late developmental stages (Fig. 2c). In those samples, 390 genes were differentially expressed in all three comparisons (Figs 2c, S3; Dataset S1).

In the differential expression analysis, we used the *P. abies* v.1.0 cDNAs as a reference (Sundell *et al.*, 2015). In this assembly, known transcripts frequently map to several scaffolds due to assembly fragmentation. For example, the transcript of the MADS-box gene *DAL10* (Carlsbecker *et al.*, 2003) (GenBank accession no. AF064080) maps in 5' to 3' direction to four ConGenIE scaffolds: MA\_15122, MA\_18073, MA\_121040, and MA\_86473g0010 (Sundell *et al.*, 2015). To connect different ConGenIE scaffolds we performed a *de novo*

transcriptome assembly using a novel assembly tool, CLUSTRAST (Westrin *et al.*, 2022). We used the assembly to connect scaffolds that mapped to the same transcript. This reduced the list of differentially expressed transcripts to 461 in the meristem samples and to 352 in the primordia samples (Dataset S2a,b). Fifty-five genes were differentially expressed in both meristem and primordia samples. Out of these, 14 genes were upregulated in *acrocona* transition shoots, female *acrocona*, and female wild-type shoots, as compared wild-type vegetative leading shoots (Table 1). We verified the upregulation of these 14 genes in female cones from four additional wild-type genotypes (Fig. S4).

### Three transcription factors were commonly upregulated in *acrocona* transition shoots and female shoots

We were primarily interested in transcription factors that may influence the shift from vegetative to reproductive shoot identity. The most significantly differentially expressed candidate among the 14 upregulated genes, MA\_15381g0010, encoded a

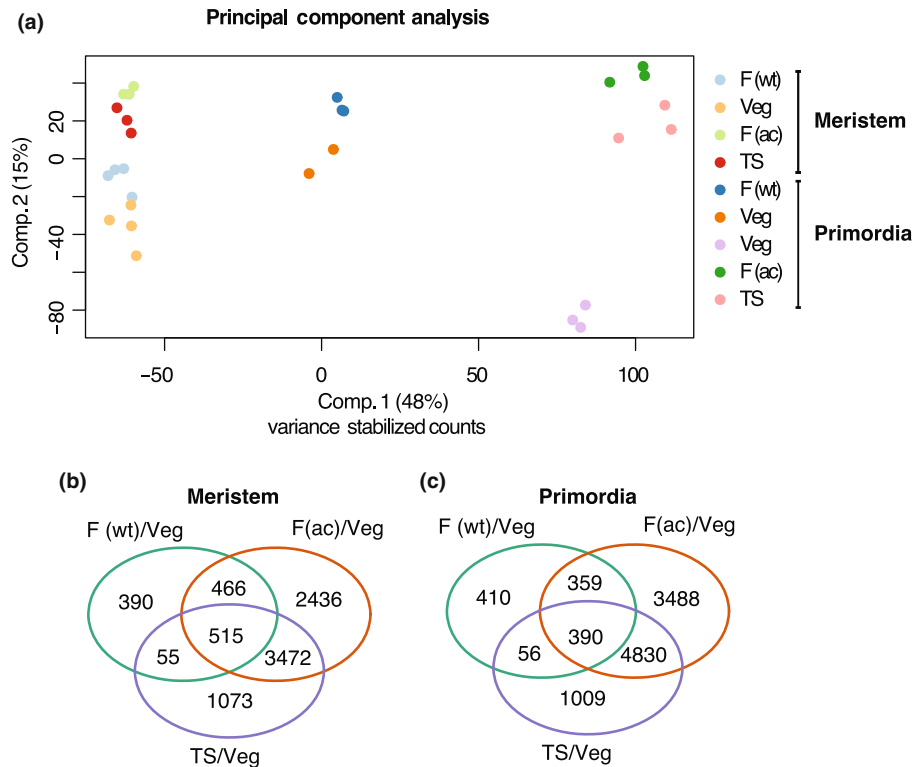


**Fig. 2** Transcriptome sequencing of *acrocona* transition shoots. (a) Principal component analysis of RNA-sequencing data from 27 samples. The first and second principal components (PC1 and PC2) define the x- and y-axes of the two-dimensional space, respectively. PC1 represents 48%, and PC2 represents 15% of the total variation in the samples. Coloured dots represent wild-type and *acrocona* samples of different bud types, in bud meristem and primordia samples. F(ac), *acrocona* female sample; F(wt), wild-type female sample; TS, *acrocona* transition shoot sample; Veg, wild-type vegetative sample. (b) Venn diagram representing differentially expressed genes (DEGs) in meristem samples collected during the early growth phase in summer, whereas the Venn diagram in (c) shows the distribution of DEGs in primordia samples collected during the late growth phase in the autumn. The green circles represent DEGs between female wild-type samples and vegetative samples (F(wt)/Veg). The orange circles represent DEGs between female *acrocona* samples and vegetative samples (F(ac)/Veg). The violet circles represent DEGs between *acrocona* transition shoot samples and vegetative samples (TS/Veg). The threshold to judge the significance of gene expression differences was false discovery rate (FDR)  $\leq 0.01$  and the absolute value of  $\log_2$ FoldChange ( $\log_2$ FC)  $\geq 0.5$ .

**Table 1** Commonly upregulated transcripts in *Picea abies* reproductive meristems and primordia.

Scaffold ID	Common name	Pfam-domains/gene family	P-value adj. (F(wt)/Veg)
MA_15381	<i>PaSPL1</i>	PF03110-SBP domain/ <i>SPL</i> -gene family	0
MA_22749	<i>PaSPL1</i>	<i>SPL</i> -gene family (C-terminal)	6.4e-260
MA_381942		Unknown	1.8e-59
MA_10430758		PF03330-Rare lipoprotein A	4.8e-53
MA_10428213		PF00135-Carboxylesterase family	2.0e-38
MA_63231		PF00044-Glyceraldehyde 3-phosphate dehydrogenase	3.7e-35
MA_65113		PF12481-Aluminium induced protein	8.9e-33
MA_86473	<i>DAL10</i>	PF00319-MADS-domain transcription factor (C-terminal)	2.0e-32
MA_194736	<i>FT-like</i>	PF01161-Phosphatidylethanolamine-binding protein	2.3e-12
MA_210262		PF00538-linker histone H1 and H5 family	1.0e-11
MA_10427625		PF01658-Myo-inositol-1-phosphate synthase	6.2e-11
MA_10436587		PF06200-tify domain	1.7e-10
MA_210555		PF00485-Phosphoribulokinase / Uridine kinase family	9.9e-08
MA_941055		PF00397-WW domain	0.0007
MA_10197498		PF00578-AhpC/TSA family	0.003

F, female cone; Veg, vegetative shoot.

transcription factor belonging to the *SPL*-gene family (Table 1). Notably, in our *de novo* transcriptome-wide assembly we were able to connect MA\_15381g0010 (on ConGenIE scaffold

MA\_15381) and the second most significant gene, MA\_22749g0010 (on ConGenIE scaffold MA\_22749), into a single transcript (ClusTrast ID 9986\_s\_0\_0) suggesting that

they are in fact part of the same gene. We named this gene *P. abies* *SQUAMOSA BINDING PROTEIN-LIKE1* (*PaSPL1*). MA\_15381g0010 harbours the signature domain of the *SPL*-gene family (Pfam domain PF03110) and MA\_22749g0010 harbours a conserved *miRNA156* binding site commonly found in *SPL*-genes, as well as a binding site for *miRNA529* (Fig. 3a). To find independent proof of the connection between MA\_15381g0010 and MA\_22749 g0010 we PCR-amplified and Sanger-sequenced the corresponding full-length cDNA clone (Fig. S5). Next, we confirmed the upregulation of *PaSPL1* in female shoots and *acrocona* transition shoots as compared to wild-type vegetative shoots using independent RT-qPCR experiments (Fig. 3b). Among the upregulated genes we detected two additional transcription factors that both belong to gene families important for flowering and floral meristem identity in angiosperms: (1) The MADS-box gene *DAL10* (MA\_86473g0010) (Fig. 3c; Table 1), suggested to be a marker for reproductive shoot identity in *P. abies* (Carlsbecker *et al.*, 2003), and (2) a previously uncharacterized *FLOWERING LOCUS T-LIKE* gene (MA\_194736g0010) belonging to the PEBP-family (Karlgrén *et al.*, 2011; Klintenas *et al.*, 2012; Liu *et al.*, 2016) of transcription factors (Table 1).

*PaSPL1* is homologous to angiosperm *SPL*-genes involved in reproductive phase change

Several publications have reported phylogenetic reconstructions of the MADS-box gene family (e.g. Carlsbecker *et al.*, 2003; Gramzow *et al.*, 2014; Akhter *et al.*, 2018). In those analyses, the *DAL10* gene commonly grouped into a gymnosperm specific sub-clade, which appears to be lost in the angiosperm lineage. In order to analyse the evolutionary relationship between conifer and angiosperm *SPL*-genes, we used the conserved SBP-domain of *PaSPL1* as bait to search for additional members of this gene family in the *P. abies* genome v.1.0 (Sundell *et al.*, 2015). In total we retrieved 10 additional members of the *SPL*-gene family from *P. abies*, here named *PaSPL2-11*. Among those, *PaSPL1*, *PaSPL2*, *PaSPL10* and *PaSPL11* harbour the conserved *miR156/529* binding site (Table S4). The evolutionary relationship between the *P. abies* *SPL*-genes and genes from the model species *A. thaliana* and *Populus trichocarpa* was analysed using Bayesian phylogenetics (Fig. S6). In this phylogeny, *PaSPL1*, *PaSPL10* and *PaSPL11* formed a clade that grouped basal to the *Arabidopsis thaliana* genes *AtSPL2*, *AtSPL6*, *AtSPL9*, *AtSPL10*, *AtSPL11* and *AtSPL15*, which all contain the *miR156* binding site, and

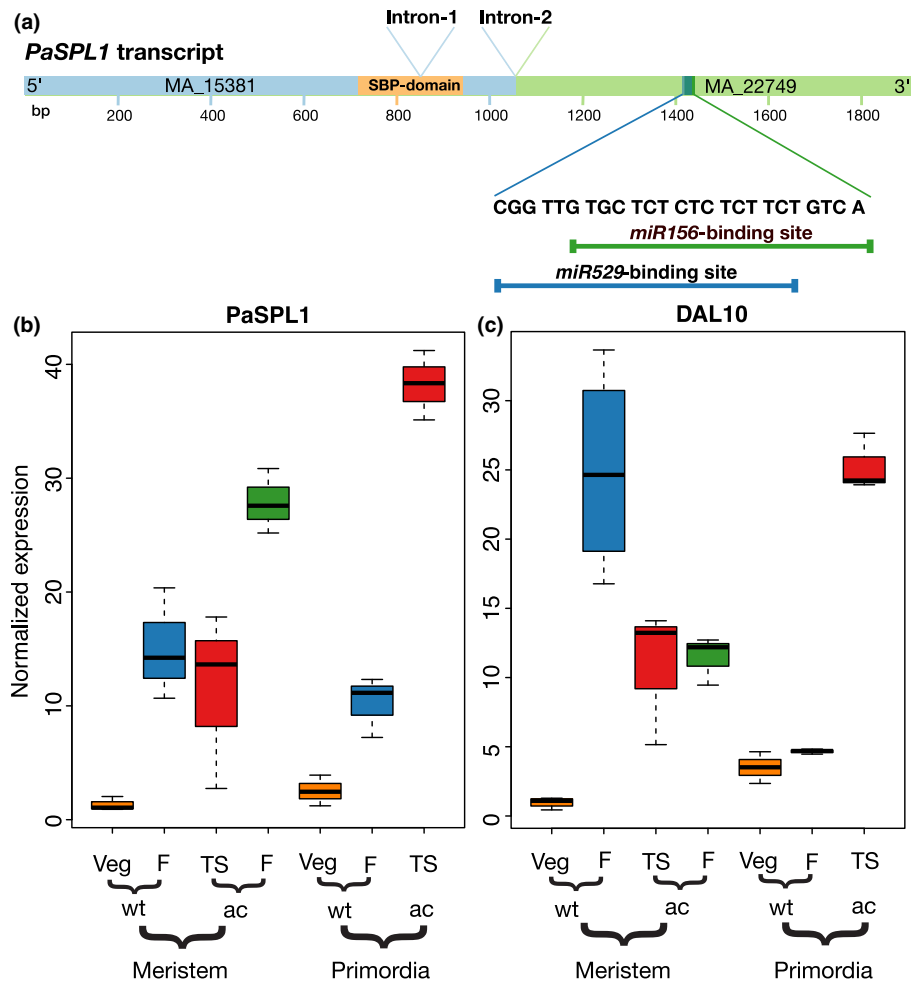


**Fig. 3** Verification of expression of *PaSPL1* and *DAL10* using reverse transcription quantitative polymerase chain reaction (RT-qPCR). (a) Graphical representation of the *PaSPL1* transcript assembled by CLUSTAL (Westrin *et al.*, 2022) with the coverage of the ConGenIE scaffolds MA\_15381 and MA\_22749 indicated in blue and green colour, respectively. Indicated are also the positions of the two introns present in the *PaSPL1* open reading frame, the signature SBP-domain and the overlapping binding sites of *miR156* and *miR529*. The boxplots in (b) and (c) show the normalized expression of *PaSPL1* and *DAL10* assayed by RT-qPCR. Veg, vegetative; F, female; TS, transition shoot; wt, wild-type; ac, *acrocona*. Box-plot elements: Line, median; box limits, upper and lower quartiles; whiskers, points.

have implicated roles in reproductive phase change (Preston & Hileman, 2013). The other *P. abies* *SPL*-genes included in the analysis grouped with other *A. thaliana* and *Populus trichocarpa* genes, e.g. *PaSPL3*, *PaSPL4* and *PaSPL5* grouped together with *AtSPL8* and *PtSPL8* (Fig. S6).

### MicroRNA156 and miR529 were upregulated in vegetative shoots and *acrocona* transition shoots

Next, we analysed the expression of miRNAs in the meristematic samples (Table S1). Illumina sequencing reads of the small RNA fraction were mapped against previously known miRNAs present in miRBase (Kozomara *et al.*, 2019). The read length of the RNA-Seq reactions allowed us to identify both precursor and mature miRNAs. We identified miRNAs with a significant difference in expression levels in at least one sample type (*acrocona* transition shoots, *acrocona* and wild-type female shoots) as compared to the same base-line sample as used in mRNA analysis (wild-type vegetative). Next, we performed hierarchical clustering of 1231 precursor and 966 mature miRNAs based on their estimated abundance levels (Figs S7, S8). Among the differentially expressed miRNAs, we identified *miR156t* and *miR529c*, which both have the capacity to bind the *PaSPL1* mRNA in a partly overlapping manner (Fig. 3a). Both *miR156t* and *miR529c* were upregulated in wild-type vegetative shoots and *acrocona* transition shoots, compared to female shoots from both genotypes (Fig. S9a,b;  $P < 0,001$ ; Dataset S3). The estimated expression levels of *miR156t* and *miR529c* were negatively correlated to the expression level of *PaSPL1* in wild-type *P. abies*, whereas *PaSPL1* and the miRNAs *miR156t* and *miR529c* were all upregulated in *acrocona* transition shoot meristems. A similar expression pattern of *miR156t* and *miR529c* was also detected in the late primordia samples (Fig. S10).

Apart from *miR156t* we also detected expression of other miRNAs that have implicated roles in the regulation of flowering or floral patterning in angiosperms (Spanudakis & Jackson, 2014), e.g. *miR159*, *miR172*, *miR167*, *miR319* and *miR390* (Figs S7, S8). Among those, *miR172* stood out as it, like *miR156t*, had a clear differential expression pattern between samples of different bud-types. In contrast to *miR156t*, *miR172i* was upregulated in female shoot meristems instead of wild-type vegetative meristems (Fig. S9c). In *acrocona* leading shoot meristems, *miR172i* had a more variable expression.

### The *acrocona* mutant harbours a SNP in the *miR156/529* binding-site of *PaSPL1*

A point mutation or a SNP in the *miR156/529* binding-site could explain the simultaneous expression of *PaSPL1*, and the miRNAs *miR156* and *miR529*, in *acrocona* transition shoots. To address this notion, we performed a separate *de novo* assembly of *PaSPL1* transcripts from either wild-type samples, or *acrocona* samples using Abeona assembly. This method can be used to identify alleles and individual SNPs in short read transcriptome datasets (Akhter *et al.*, 2018). As a reference, we performed similar allele-specific assemblies of the remaining candidate genes listed in Table 1 and four additional genes that also harbour the

*miR156/529* binding-site. Thirteen of the assembled genes had SNPs in the *acrocona* mutant background (Table S5; Dataset S4). Next, we compared SNPs present in the assembled *acrocona*-transcripts with SNPs present in the Swedish breeding population of *P. abies* (Wang *et al.*, 2020). In this comparison, only four genes had *acrocona* specific SNPs, and among those, only *PaSPL1* also had a *miR156/529* binding site (Table S5). *PaSPL1* had two *acrocona* specific SNPs, one located 256 nucleotides from the assumed start codon, and a second in the *miR156/529* binding-site at nt 1421 (Fig. 4a). Sanger sequencing of full-length cDNA

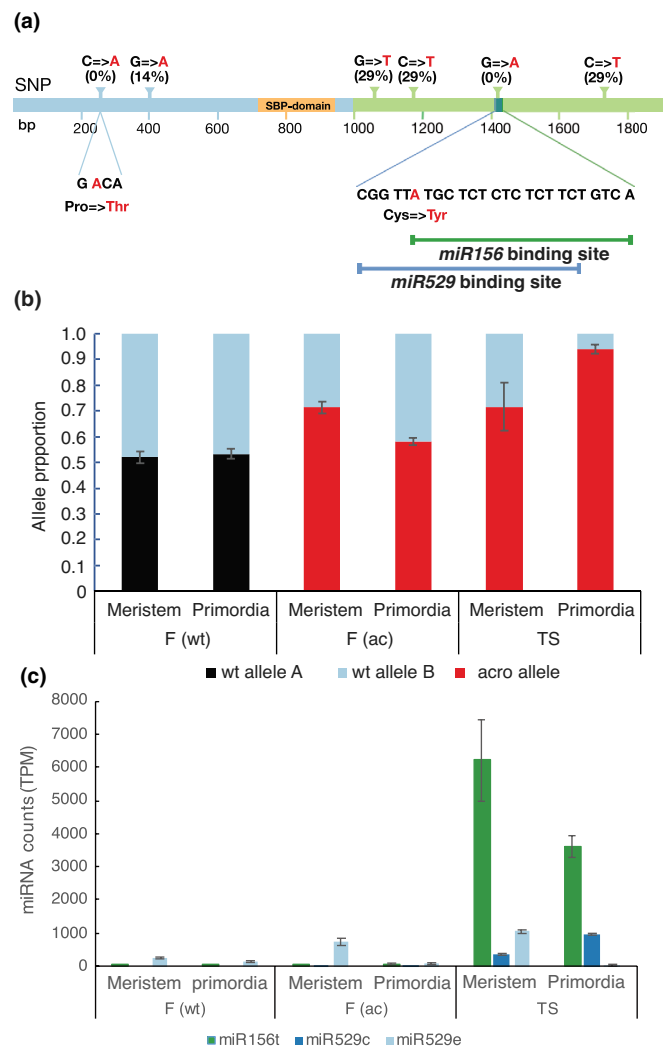


**Fig. 4** Allele specific expression of *PaSPL1*. (a) Graphical representation of the *PaSPL1* transcript. Indicated are the six single nucleotide polymorphism (SNP) positions identified in the *acrocona* allele of *PaSPL1*, the signature SBP-domain and the overlapping binding sites of *miR156* and *miR529*. Red colour indicates the substitution identified in the *acrocona* allele of *PaSPL1*. The percentage shown after each SNP indicates how common a specific SNP is in the *Picea abies* wild-type population. (b) Proportions of transcripts from the wild-type alleles and the *acrocona* allele in the different messenger RNA (mRNA) samples (c) Estimated counts (transcript per million (TPM)) of *miR156t*, *miR529c* and *miR529e*. Each column represents the mean of three biological replicates. Error-bars show standard error. Data points underlying the means are presented in Dataset S2d. F(wt), female wild-type; F(ac), female *acrocona*; TS, *acrocona* transition shoots.

clones derived from the *acrocona* and the wild-type comparator confirmed the presence of this *acro*-SNP at nucleotide 1421.

### Expression of *miR156* and *miR529* affected the allelic proportion of expressed *PaSPL1*

To test if the expression of *miR156* or *miR529* affects *PaSPL1* expression levels in an allele-specific manner, we estimated the proportion mRNA expressed from each allele in the transcriptome datasets (Fig. 4b; Dataset S2c). We also assessed *miR156* and *miR529* levels in the same samples (Fig. 4c; Dataset S2d). Wild-type female meristems and primordia expressed low levels of *miR156* and *miR529*, and the two *PaSPL1* alleles were expressed in equal proportions (Fig. 4b,c, left column). In *acrocona* female shoots, the *PaSPL1* allele proportion (*acrocona* vs wild-type) was 70 : 30 in the early meristematic samples and 50 : 50 in the later primordia samples (Fig. 4b, middle column). In the meristem samples, we observed elevated expression of an additional *miR529* variant, *miR529e*, whereas primordia samples expressed low levels of all variants of *miR156* and *miR529* (Fig. 4c, middle column). Similar to the *acrocona* females, the allele proportion in meristematic samples from transition shoots was about 70 : 30. In the later transition shoot samples, the *acro*-allele accounted for almost 95% of all *PaSPL1* transcripts (Fig. 4b, right column). As noted in our differential expression analysis of miRNAs (Fig. S9), *acrocona* transition shoots expressed elevated levels of both *miR156t* and *miR529c*, and in the early meristematic samples, *miR529e* (Fig. 4c, right column). In short, in samples that expressed elevated levels of *miR156* or *miR529*, the allele proportion of *PaSPL1* was affected in favour of the allele which harboured the *acro*-SNP. This pattern was evident in the early meristematic samples and became even more pronounced in the later primordia samples.

### *MicroR156/529* cleave *PaSPL1* in an allele specific manner

The allele-specific reduction of *PaSPL1* transcripts in *acrocona* transition shoots could be explained by *miR156/529* mediated transcript cleavage. To examine this possibility, we performed 5' RLM RACE experiments. Putative *PaSPL1* cleavage- and degradation products of the expected size (*c.* 450 bp) could be readily observed in wild-type vegetative samples and, to some extent, in samples from *acrocona* transition shoots (Fig. S11a). Quantification of short degradation products that end at, or downstream of, the *miR156/529* binding-site compared to longer general degradation products that span the entire *miR156/529* binding-site reflects this pattern (Fig. S11b). We identified two putative *PaSPL1* cleavage products from the wild-type vegetative samples by cloning and Sanger sequencing gel-purified DNA-fragments of the expected size. Seventeen out of 24 cloned fragments ended at nt 1427, i.e. within the *miR156/529* binding site, and four fragments ended at nt 1431 (Fig. S11c). By cloning and Sanger sequencing of gel-purified fragments from the *acrocona* transition shoot, we detected two longer degradation products, three additional putative cleavage products that ended at nt 1427, and several shorter *PaSPL1* fragments (Table S6). Furthermore, SNPs

present in the cloned DNA fragments showed that the long uncleaved degradation products were expressed from the *acrocona* allele. In contrast, the putative cleavage products that ended at nt 1427, and the shorter fragments, were all from the wild-type allele. This indicates that expression of *miR156* and *miR529* preferentially mediate a cleavage of the wild-type allele of *PaSPL1*, and that this cleavage could explain the differences in the expression levels of the two alleles in *acrocona* transition shoots.

### The *acro*-SNP co-segregated with the early cone-setting *acrocona* phenotype

We have previously performed inbred crosses of adult ramets of the *acrocona* mutant (Uddenberg *et al.*, 2013). One-fourth of the resulting siblings displayed an enhanced early cone-setting phenotype and produced cones during the third growth cycle. As these trees have grown older, they now form rounded bushes with no clear apical dominance and regularly produce transition shoots on almost every shoot (Fig. S12). We expect that the causal mutation for the *acrocona* phenotype should be homozygous for the *acro*-allele in the early cone-setting siblings. To test if any of our candidate genes met this criterion, we analysed the segregation pattern of the *acro*-specific SNPs identified in the genes *PaSPL1*, MA\_381942g0010, MA\_10436587g0010 and MA\_21055g010 in a sub-set of trees from the sibling population (Table S7). In this analysis only *PaSPL1* was homozygous for its *acro*-specific SNP in early cone-setting trees.

To provide further support for this segregation pattern, we genotyped the entire segregating inbred sibling population generated in Uddenberg *et al.* (2013) (Table 2; Dataset S2e). In this analysis, 32% of the segregating sibling trees were homozygous for the *acro*-SNP present in *PaSPL1*, 57% were heterozygous, and 11% homozygous wild-type. Among the sibling trees that were homozygous for the *acro*-SNP, 92% displayed either an early cone-setting (21/24) or an intermediate *acrocona* (1/24) phenotype. Only two homozygous trees produced vegetative topshoots, and both of those trees had stunted growth. All heterozygous trees (42/42) produced vegetative shoots only. Similarly, none of the trees that were homozygous wild-type had any cones. Hence, we detected a highly significant ( $P < 0.00001$ , Fisher's exact test) correlation between trees homozygous for the *acro*-SNP and the early cone-setting phenotype.

We also genotyped wild stands of the *acrocona* mutant which all displayed a semidominant phenotype (Fig. S13). All trees were heterozygous with respect to the *acro*-SNP (Table S8; Dataset S2f), whereas two of the trees were also homozygous for the upstream *acrocona* specific SNP at nucleotide 256 (Dataset S2f). This

**Table 2** Genotyping of inbred *Picea abies* var. *acrocona* siblings.

Genotype/phenotype	Wt (G/G)	Het (G/A)	acro (AA)
Apical cone	0	0	21 (88%)
Intermediate	0	0	1 (4%)
Vegetative	8 (100%)	43 (100%)	2 (8%)
Total	8	43	24

suggests that the upstream SNP is not necessary for the enhanced phenotype displayed by homozygous *acrocona* plants.

## Discussion

In most of Sweden's planting zones, there is a shortage of domestically produced *P. abies* seeds (Rosvall, 2011). This shortage has two primary causes: irregular cone-setting of *P. abies* and damages to cones and seeds caused by insects and fungi (Almqvist *et al.*, 2010). Conifer breeding and research also face a significant obstacle because of the very long generation times (Flachowsky *et al.*, 2009). Therefore, there is a strong desire to learn more about the molecular mechanism that regulates cone-setting in conifers (Uddenberg *et al.*, 2015). Understanding the genetic mechanism that regulates reproductive phase change in conifers could also increase our understanding of the evolutionary relationship between extant seed plants, i.e. angiosperms and gymnosperms.

In this study, we utilized the unique features of an adult, naturally occurring and presumably heterozygous, *acrocona* mutant. In this *acrocona* mutant, apical shoots on leading branches commonly develop into transition shoots. Like vegetative shoots, the first lateral organs that initiate in *acrocona* transition shoots are needles. Later in the growing season, the *acrocona* transition shoots produce ovuliferous scale-like structures. Hence, we collected samples that allowed us to identify genes expressed in the *acrocona* transition shoots before any morphological signs of the reproductive shift were apparent, and we compared their transcriptome profiles to profiles generated from corresponding wild-type vegetative shoot meristems and female meristems. This selection of shoots allowed us to address the hypothesis that the *acrocona* transition shoots express genes related to reproductive shoot development before the morphological shift. It was also likely that the identified candidate genes would be active in the meristem rather than acting in the down-stream morphological differentiation. Genes upregulated in both transition shoots and female meristems of *acrocona* (relative to wild-type vegetative meristems) would therefore be candidates for genes important for reproductive meristem identity.

Apart from the meristematic samples collected in early August, we also collected primordia samples during the autumn, when lateral organ differentiation occurs. In this growth phase, vascular strands connect to the lateral organs and cellular differentiation occurs within the ovuliferous scales and sterile bracts in female cones, and within the needles in vegetative shoots. Similar cellular differentiation also occurs in the *acrocona* transition shoots.

By combining the results from comparisons of meristem and primordia samples, we identified 14 genes that were upregulated in *acrocona* transition shoots and female cones as compared to wild-type vegetative leading shoots. In line with the hypothesis that these 14 genes represent genes important for reproductive development, we identified *DAL10*, a marker for reproductive shoot identity (Carlsbecker *et al.*, 2003). Among the top candidate genes, we also identified a member of the *SPL* gene family, here named *PaSPL1*. In our phylogenetic analysis of the *SPL* gene family, *PaSPL1* groups together with angiosperm *SPL*-genes that

have been shown to regulate flowering (Preston & Hileman, 2013). This is interesting because a certain position in a phylogenetic tree may be indicative not only of shared ancestry, but also of conserved function between closely located genes (Theissen *et al.*, 1996; Tandre *et al.*, 1998). Although sub-functionalization and neo-functionalization frequently occur (Irish & Litt, 2005).

In angiosperms, members of the *SPL*-gene family are key regulators of the age-dependent flowering pathway (Wang *et al.*, 2009; Preston & Hileman, 2013). This pathway also includes *miR156*, which acts as a negative regulator of the *SPL*-genes during juvenile stages and in vegetative meristems. Expression of *miR156*-resistant variants of *AaSPL15* in the perennial herb *A. alpina* is known to induce early flowering and flowering in positions which in wild-type would continue as vegetative shoots (Hyun *et al.*, 2019). We note that this resembles the *acrocona* mutant phenotype. Analysis of the *PaSPL1* sequence revealed that *PaSPL1* harbours a conserved *miR156* binding site located 1421 nucleotides downstream from the start codon. Partly overlapping was also the binding site of *miR529*, a miRNA that has been lost in the core eudicots but that is still present in, e.g. bryophytes and monocots such as *Oryza sativa* (Morea *et al.*, 2016). The occurrence of an overlapping binding site indicates that both miRNAs may negatively regulate *PaSPL1*. In line with this hypothesis, we detected an elevated expression of both *miR156* and *miR529* in wild-type vegetative leading meristem compared with female meristems of both assayed genotypes. This supports the hypothesis that the *SPL/miR156* module of the age-dependent flowering pathway regulates reproductive phase change in conifers – possibly with the additional involvement of *miR529*.

Interestingly, both *miR156* and *miR529* were co-expressed with *PaSPL1* in *acrocona* transition shoot meristems. The SNP present in the overlapping *miR156/529* binding site of the *PaSPL1* *acrocona* allele could explain the co-expression: we detected (1) two distinct cleavage products of *PaSPL1* in samples from vegetative shoots cleaved in the putative *miR156/529* target site, (2) specific cleavage of the wild-type allele of *PaSPL1* in heterozygous *acrocona* transition shoots, and (3) a higher expression of the *acrocona* allele (as compared to the wild-type allele) in *acrocona* transition shoots. This indicates that *miR156* and/or *miR529* can mediate *PaSPL1* cleavage, and that this cleavage occurs in an allele specific manner, suggesting that the *acro*-SNP renders the *acrocona* allele *miR156/529* tolerant. We note that similar dual cleavage products of *SPL* transcripts have been reported previously in heterologous experiments studying the ectopic expression of *miR156* and *miR529* from *O. sativa* in *A. thaliana* (Morea *et al.*, 2016).

Provided that *PaSPL1* regulates female reproductive identity, we would expect a co-segregation of this SNP with the *acrocona* phenotype. Indeed, the *acro*-SNP is absent in a tested set of 35 wild-type genotypes that are part of the Swedish breeding population (Wang *et al.*, 2020). In our previous studies, we have produced an inbred population of the *acrocona* mutant. One quarter segregated with an early cone-setting phenotype among the sibling trees, which we then interpreted as an enhanced homozygous phenotype (Uddenberg *et al.*, 2013). As these plants have grown

older, they only became rounded shrubs, distinct from the heterozygous *acrocona* trees, which displayed a semi-dominant phenotype and grew taller. We have now demonstrated a co-segregation between the early cone-setting phenotype and trees that are homozygous for the *acro*-SNP by genotyping. Importantly, none of the segregating siblings that were homozygous for the wild-type allele displayed any *acrocona* phenotypes.

In conclusion, we propose that cone-setting in the conifer *P. abies* is regulated by conserved elements of the age-dependent flowering pathway. In support of this notion, we provide several independent lines of experimental evidence: (1) Using transcriptome analyses, we demonstrate an anti-correlated expression of *PaSPL1* and *miR156/529* in female and vegetative shoot meristems. (2) Using allele-specific assembly and expression analysis, we identify an *acrocona* specific SNP in the miRNA binding site of *PaSPL1*. We show that the *acrocona* allele of *PaSPL1* is upregulated in transition shoots, along with *miR156* and *miR529* in contrast to the anti-correlated expression in wild-type shoots. (3) Using RLM RACE experiments, we show that *miR156* and *miR529* preferentially mediate cleavage of the wild-type allele of *PaSPL1*. (4) Finally, we demonstrate that among our *acrocona* specific SNPs—in *PaSPL1* and other candidate genes—only the *acro*-SNP in the miRNA binding site of *PaSPL1* co-segregates with the enhanced *acrocona* phenotype. We have, however, not analysed the genomic sequence of *PaSPL1*, and it is possible that other unknown SNPs or perhaps the SNP located at nucleotide 256 in the *PaSPL1* transcript also contribute to the *acrocona* phenotype. Considering these numerous lines of evidence, together with the similarity to the situation in the angiosperm perennial herb *Arabis alpina*, the most parsimonious conclusion is that the early flowering of the *acrocona* mutant is caused by the mutation in the *miR156/miR529* binding site of the *PaSPL1* gene. However, to ultimately prove that the *acro*-SNP alone is responsible for the *acrocona* phenotype we would be required to find, or generate, independent mutations in the *PaSPL1* locus. Our results demonstrate remarkable conservation of this pathway, which is linked to perennity, between species that shared a last common ancestor 300 million years ago. Hence, the age-dependent pathway seems to be crucial to the regulation of reproductive phase change not only in conifers, but also in many other perennial seed plants.

## Acknowledgements

The authors acknowledge funding for salaries and consumables from the Carl Tryggers Foundation (grant number CTS 18:367), the Royal Physiographic Society (22309-000), the Swedish Foundation for Strategic Research (FID16-0030 and FFF20-0014), Formas (239-2013-650 and 2021 01026), and by grants from the SLU Plant Breeding platform and Trees and Crops for the Future (TC4F). The computations were enabled by resources in project SNIC 2017/7-303 provided by the Swedish National Infrastructure for Computing (SNIC) at UPPMAX and project PDC-2020-43 at Paralleldatorcentrum (PDC), partially funded by the Swedish Research Council (grant no. 2018-05973).

## Author contributions

JFS and OE planned and designed the research. JFS wrote the manuscript with contributions from SA, KJW and NZ. SA, NZ and VN performed the experiments and conducted fieldwork. SA, KJW, WWK and ND analysed the data. JFS, OE, NRS and ON provided supervision, funding and materials. All authors read and edited the final version of the manuscript. SA, KJW and NZ contributed equally to this work. JFS and OE are the joint corresponding authors on the manuscript.

## ORCID

Shirin Akhter  <https://orcid.org/0000-0003-4238-3110>  
Nicolas Delhomme  <https://orcid.org/0000-0002-3053-0796>  
Olof Emanuelsson  <https://orcid.org/0000-0002-8879-9245>  
Warren W. Kretzschmar  <https://orcid.org/0000-0002-2575-0807>  
Ove Nilsson  <https://orcid.org/0000-0002-1033-1909>  
Nathaniel R. Street  <https://orcid.org/0000-0001-6031-005X>  
Jens F. Sundström  <https://orcid.org/0000-0003-2848-5284>  
Karl Johan Westrin  <https://orcid.org/0000-0002-6937-9245>

## Data availability

All data generated or analysed during this study are included in this published article or its Supporting Information. The sequencing data is available at the European Nucleotide Archive (ENA, <https://www.ebi.ac.uk/ena/browser/home>) under the accession no. PRJEB45942. All custom-made code is available at either <https://github.com/karljohanw/clustrast> or <https://github.com/winni2k/abeona>.

## References

- Akhter S, Kretzschmar WW, Nordal V, Delhomme N, Street NR, Nilsson O, Emanuelsson O, Sundstrom JF. 2018. Integrative analysis of three RNA sequencing methods identifies mutually exclusive exons of MADS-box isoforms during early bud development in *Picea abies*. *Frontiers in Plant Science* **9**: 1625.
- Albani MC, Coupland G. 2010. Comparative analysis of flowering in annual and perennial plants. *Current Topics in Developmental Biology* **91**: 323–348.
- Almqvist C, Wennström U, Karlsson B. 2010. *Förädlad skogsodlingsmaterial 2010–2050. Tillgång och behov av förädlad frö samt förslag på åtgärder för att minimera brist och maximera genetisk vinst*. Uppsala, Sweden: Skogforsk.
- Azevedo H, Lino-Neto T, Tavares RM. 2003. An improved method for high-quality RNA isolation from needles of adult maritime pine trees. *Plant Molecular Biology Reporter* **21**: 333–338.
- Blazquez MA, Weigel D. 2000. Integration of floral inductive signals in Arabidopsis. *Nature* **404**: 889–892.
- Bolger AM, Lohse M, Usadel B. 2014. Trimmomatic: a flexible trimmer for Illumina sequence data. *Bioinformatics* **30**: 2114–2120.
- Bray NL, Pimentel H, Melsted P, Pachter L. 2016. Near-optimal probabilistic RNA-seq quantification. *Nature Biotechnology* **34**: 525–527.
- Carlsbecker A, Sundstrom J, Tandere K, Englund M, Kvarnheden A, Johanson U, Engstrom P. 2003. The DAL10 gene from Norway spruce (*Picea abies*) belongs to a potentially gymnosperm-specific subclass of MADS-box genes and is specifically active in seed cones and pollen cones. *Evolution & Development* **5**: 551–561.
- Carlsbecker A, Sundstrom JF, Englund M, Uddenberg D, Izquierdo L, Kvarnheden A, Vergara-Silva F, Engstrom P. 2013. Molecular control of

- normal and *acrocona* mutant seed cone development in Norway spruce (*Picea abies*) and the evolution of conifer ovule-bearing organs. *New Phytologist* 200: 261–275.
- Chen S, Zhou Y, Chen Y, Gu J. 2018. FASTP: an ultra-fast all-in-one FASTQ preprocessor. *Bioinformatics* 34: i884–i890.
- Crisuolo A, Gribaldo S. 2010. BMGE (Block Mapping and Gathering with Entropy): a new software for selection of phylogenetic informative regions from multiple sequence alignments. *BMC Evolutionary Biology* 10: 210.
- Flachowsky H, Hanke MV, Peil A, Strauss SH, Fladung M. 2009. A review on transgenic approaches to accelerate breeding of woody plants. *Plant Breeding* 128: 217–226.
- Florin R. 1951. Evolution in cordaites and conifers. *Acta Horti Bergiani* 15: 285–388.
- Futamura N, Igasaki T, Saito M, Taira H, Shinohara K. 2019. Comparison of fertile and sterile male gametogenesis in *Cryptomeria japonica* D. Don. *Tree Genetics & Genomes* 15: 30.
- Gentleman RC, Carey VJ, Bates DM, Bolstad B, Dettling M, Dudoit S, Ellis B, Gautier L, Ge Y, Gentry J *et al.* 2004. BIOCONDUCTOR: open software development for computational biology and bioinformatics. *Genome Biology* 5: R80.
- Giacomello S, Salmen F, Terebieniec BK, Vickovic S, Navarro JF, Alexeyenko A, Reimegard J, McKee LS, Mannapperuma C, Bulone V *et al.* 2017. Spatially resolved transcriptome profiling in model plant species. *Nature Plants* 3: 17061.
- Gramzow L, Weilandt L, Theissen G. 2014. MADS goes genomic in conifers: towards determining the ancestral set of MADS-box genes in seed plants. *Annals of Botany* 114: 1407–1429.
- Huelsenbeck JP, Ronquist F. 2001. MRBAYES: Bayesian inference of phylogenetic trees. *Bioinformatics* 17: 754–755.
- Hyun Y, Vincent C, Tilmes V, Bergonzi S, Kiefer C, Richter R, Martinez-Gallegos R, Severing E, Coupland G. 2019. A regulatory circuit conferring varied flowering response to cold in annual and perennial plants. *Science* 363: 409–412.
- Irish VF, Litt A. 2005. Flower development and evolution: gene duplication, diversification and redeployment. *Current Opinion in Genetics & Development* 15: 454–460.
- Karlgen A, Gyllenstrand N, Kallman T, Sundstrom JF, Moore D, Lascoux M, Lagercrantz U. 2011. Evolution of the PEBP gene family in plants: functional diversification in seed plant evolution. *Plant Physiology* 156: 1967–1977.
- Kim CS, Lee CH, Shin JS, Chung YS, Hyung NI. 1997. A simple and rapid method for isolation of high quality genomic DNA from fruit trees and conifers using PVP. *Nucleic Acids Research* 25: 1085–1086.
- Klintonas M, Pin PA, Benlloch R, Ingvarsson PK, Nilsson O. 2012. Analysis of conifer *FLOWERING LOCUS T/TERMINAL FLOWER1*-like genes provides evidence for dramatic biochemical evolution in the angiosperm FT lineage. *New Phytologist* 196: 1260–1273.
- Kopylova E, No L. 2012. SORTMERA: fast and accurate filtering of ribosomal RNAs in metatranscriptomic data. *Bioinformatics* 28: 3211–3217.
- Kozomara A, Birgaoanu M, Griffiths-Jones S. 2019. miRBase: from microRNA sequences to function. *Nucleic Acids Research* 47(D1): D155–D162.
- Li H. 2018. MINIMAP2: pairwise alignment for nucleotide sequences. *Bioinformatics* 34: 3094–3100.
- Lindgren K, Ekberg I, Eriksson G. 1977. External factors influencing female flowering in *Picea abies* (L.) Karst. *Studia Forestalia Suecica* 142: 1–53.
- Liu YY, Yang KZ, Wei XX, Wang XQ. 2016. Revisiting the phosphatidylethanolamine-binding protein (PEBP) gene family reveals cryptic *FLOWERING LOCUS T* gene homologs in gymnosperms and sheds new light on functional evolution. *New Phytologist* 212: 730–744.
- Llave C, Franco-Zorrilla JM, Solano R, Barajas D. 2011. Target validation of plant microRNAs. *Methods in Molecular Biology* 732: 187–208.
- Love MI, Huber W, Anders S. 2014. Moderated estimation of fold change and dispersion for RNA-seq data with DESeq2. *Genome Biology* 15: 550.
- Morea EGO, da Silva EM, e Silva GFF, Valente GT, Barrera Rojas CH, Vincenz M, FTS N. 2016. Functional and evolutionary analyses of the *miR156* and *miR529* families in land plants. *BMC Plant Biology* 16: 40.
- Mouradov A, Hamdorf B, Teasdale RD, Kim JT, Winter KU, Theissen G. 1999. A *DEF/GLO*-like MADS-box gene from a gymnosperm: *Pinus radiata* contains an ortholog of angiosperm B class floral homeotic genes. *Developmental Genetics* 25: 245–252.
- Muller PY, Janovjak H, Miserez AR, Dobbie Z. 2002. Processing of gene expression data generated by quantitative real-time RT-PCR. *Biotechniques* 32: 1372–1374 1376, 1378–1379.
- Niu S, Yuan H, Sun X, Porth I, Li Y, El-Kassaby YA, Li W. 2016. A transcriptomics investigation into pine reproductive organ development. *New Phytologist* 209: 1278–1289.
- Niu S, Yuan L, Zhang Y, Chen X, Li W. 2014. Isolation and expression profiles of gibberellin metabolism genes in developing male and female cones of *Pinus tabulaeformis*. *Functional & Integrative Genomics* 14: 697–705.
- O'Maoileidigh DS, Graciet E, Wellmer F. 2014. Gene networks controlling *Arabidopsis thaliana* flower development. *New Phytologist* 201: 16–30.
- Pimentel H, Bray NL, Puente S, Melsted P, Pachter L. 2017. Differential analysis of RNA-seq incorporating quantification uncertainty. *Nature Methods* 14: 687–690.
- Preston JC, Hileman LC. 2013. Functional evolution in the plant *SQUAMOSA-PROMOTER BINDING PROTEIN-LIKE (SPL)* gene family. *Frontiers in Plant Science* 4: 80.
- R\_Core\_Team. 2013. *R: A language and environment for statistical computing*. Vienna, Austria: R Foundation for Statistical Computing.
- Rosvall O. 2011. *Review of the Swedish tree breeding programme*. Uppsala, Sweden: Skogforsk.
- Rutledge R, Regan S, Nicolas O, Fobert P, Cote C, Bosnich W, Kauffeldt C, Sunohara G, Seguin A, Stewart D. 1998. Characterization of an *AGAMOUS* homologue from the conifer black spruce (*Picea mariana*) that produces floral homeotic conversions when expressed in *Arabidopsis*. *The Plant Journal* 15: 625–634.
- Sanger F, Nicklen S, Coulson AR. 1977. DNA sequencing with chain-terminating inhibitors. *Proceedings of the National Academy of Sciences, USA* 74: 5463–5467.
- Sauquet H, von Balthazar M, Magallon S, Doyle JA, Endress PK, Bailes EJ, de Moraes EB, Bull-Herenu K, Carrive L, Chartier M *et al.* 2017. The ancestral flower of angiosperms and its early diversification. *Nature Communications* 8: 10.
- Schurch NJ, Schofield P, Gierlinski M, Cole C, Sherstnev A, Singh V, Wrobel N, Gharbi K, Simpson GG, Owen-Hughes T *et al.* 2016. How many biological replicates are needed in an RNA-seq experiment and which differential expression tool should you use? *RNA* 22: 839–851.
- Smith SA, Beaulieu JM, Donoghue MJ. 2010. An uncorrelated relaxed-clock analysis suggests an earlier origin for flowering plants. *Proceedings of the National Academy of Sciences, USA* 107: 5897–5902.
- Soneson C, Love MI, Robinson MD. 2015. Differential analyses for RNA-seq: transcript-level estimates improve gene-level inferences. *F1000Research* 4: 1521.
- Spanudakis E, Jackson S. 2014. The role of microRNAs in the control of flowering time. *Journal of Experimental Botany* 65: 365–380.
- Sundell D, Mannapperuma C, Netotea S, Delhomme N, Lin Y-C, Aa S. 2015. The plant genome integrative explorer resource: PlantGenIE.org. *New Phytologist* 208: 1149–1156.
- Sundstrom J, Carlsbecker A, Svensson ME, Svenson M, Johanson U, Theissen G, Engstrom P. 1999. MADS-box genes active in developing pollen cones of Norway spruce (*Picea abies*) are homologous to the B-class floral homeotic genes in angiosperms. *Developmental Genetics* 25: 253–266.
- Tandre K, Svenson M, Svensson ME, Engstrom P. 1998. Conservation of gene structure and activity in the regulation of reproductive organ development of conifers and angiosperms. *The Plant Journal* 15: 615–623.
- Theissen G, Kim JT, Saedler H. 1996. Classification and phylogeny of the MADS-box multigene family suggest defined roles of MADS-box gene subfamilies in the morphological evolution of eukaryotes. *Journal of Molecular Evolution* 43: 484–516.
- Turner I, Garimella KV, Iqbal Z, McVean G. 2018. Integrating long-range connectivity information into de Bruijn graphs. *Bioinformatics* 34: 2556–2565.

- Uddenberg D, Akhter S, Ramachandran P, Sundstrom JF, Carlsbecker A. 2015. Sequenced genomes and rapidly emerging technologies pave the way for conifer evolutionary developmental biology. *Frontiers in Plant Science* 6: 970.
- Uddenberg D, Reimegard J, Clapham D, Almqvist C, von Arnold S, Emanuelsson O, Sundstrom JF. 2013. Early cone setting in *Picea abies* *acrocona* is associated with increased transcriptional activity of a MADS box transcription factor. *Plant Physiology* 161: 813–823.
- Wang JW, Czech B, Weigel D. 2009. miR156-regulated SPL transcription factors define an endogenous flowering pathway in *Arabidopsis thaliana*. *Cell* 138: 738–749.
- Wang X, Bernhardsson C, Ingvarsson PK. 2020. Demography and natural selection have shaped genetic variation in the widely distributed conifer Norway spruce (*Picea abies*). *Genome Biology and Evolution* 12: 3803–3817.
- Westrin KJ, Kretzschmar WW, Emanuelsson O. 2022. CLUSTRAST: a short read de novo transcript isoform assembler guided by clustered contigs. *bioRxiv*. doi: 10.1101/2022.01.02.473666.
- Winter KU, Becker A, Munster T, Kim JT, Saedler H, Theissen G. 1999. MADS-box genes reveal that gnetophytes are more closely related to conifers than to flowering plants. *Proceedings of the National Academy of Sciences, USA* 96: 7342–7347.

## Supporting Information

Additional Supporting Information may be found online in the Supporting Information section at the end of the article.

**Dataset S1** Differentially expressed genes.

**Dataset S2** Background data.

**Dataset S3** MicroRNA statistics.

**Dataset S4** Consensus *acrocona* transcripts.

**Fig. S1** Genotyping of the *acro*-single nucleotide polymorphism in *PaSPL1*.

**Fig. S2** Hierarchical clustering of differentially expressed genes in early meristematic samples.

**Fig. S3** Hierarchical clustering of differentially expressed genes in late primordia samples.

**Fig. S4** Expression of candidate genes in control samples.

**Fig. S5** Cloning and sequencing of the *PaSPL1* coding sequence.

**Fig. S6** SQUAMOSA BINDING PROTEIN-LIKE (SPL) gene family phylogeny.

**Fig. S7** Hierarchical clustering of precursor microRNA expressed in meristem.

**Fig. S8** Hierarchical clustering of mature microRNAs expressed in meristems.

**Fig. S9** Expression of *miR156t*, *miR529c*, and *miR172i*.

**Fig. S10** Hierarchical clustering of mature microRNAs expressed in bud primordia.

**Fig. S11** *PaSPL1* transcript cleavage estimated by 5' RNA Ligase-Mediated 5' Rapid Amplification of cDNA Ends (5' RLM RACE).

**Fig. S12** Phenotypes of inbred *acrocona* siblings after 13 growth-cycles.

**Fig. S13** Locations and phenotypes of adult stands of *acrocona* trees.

**Table S1** Samples subjected to RNA-sequencing.

**Table S2** Primers used in the study.

**Table S3** Samples used in 5' RNA Ligase-Mediated 5' Rapid Amplification of cDNA Ends (5' RLM RACE) experiments.

**Table S4** The *PaSPL*-gene family.

**Table S5** *Acrocona* specific single nucleotide polymorphisms.

**Table S6** Frequency of RNA Ligase-Mediated 5' Rapid Amplification of cDNA Ends (5' RLM RACE) products.

**Table S7** Genotyping of genes with *acrocona* specific single nucleotide polymorphisms.

**Table S8** Genotyping of adult stands of *acrocona* and wild-type *Picea abies*.

Please note: Wiley Blackwell are not responsible for the content or functionality of any Supporting Information supplied by the authors. Any queries (other than missing material) should be directed to the *New Phytologist* Central Office.